

# Model-Based Leakage Detection in a Pulverized Coal Injection Vessel

Andreas Johansson, *Student Member, IEEE*, and Alexander Medvedev

**Abstract**—A method for detecting and isolating incipient leakages in the valves of a pulverized coal injection vessel for a blast furnace process is presented. Nonlinear physical gray-box models of the plant are developed. Values of the unknown parameters are estimated by identification. Observers are constructed for these models and the residuals are used in a generalized likelihood ratio test. The method is successfully tested with real leakages intentionally introduced in the plant.

**Index Terms**—Fault detection and isolation, gas leakage detection, nonlinear observers, pulverized coal injection, valves.

## NOMENCLATURE

$a_C, a_N$	Parameters of the pressurization and injection process.
$c_P$	Exponential coefficient of the pressure control valve (PCV) characteristic.
$d_F, d_P$	Deadzones of the flow control valve (FCV) and PCV.
$k_0, k_1$	Parameters of the ventilation process.
$k_{C,F}, k_{N,F}, k_{N,P}$	Parameters of the pressurization and injection process.
$m$	Total mass in the vessel.
$m_C, m_N$	Masses of coal and nitrogen in the vessel.
$p$	Pressure in the vessel.
$p_A, p_I, p_N$	Pressure of the atmosphere, injection pipe, and nitrogen net.
$q_{C,F}$	Mass flow of coal through the FCV.
$q_L, \hat{q}_L$	Real and approximated leakage flow.
$q_{N,F}, q_{N,P}, q_{N,V}$	Mass flow of nitrogen through the FCV, PCV, and VV.
$R_N$	Gas constant for nitrogen.
$\rho_C$	Density of coal.
$T$	Temperature in the vessel.
$u_F, u_P$	Control signal for the FCV and the PCV.
$V$	Volume of the vessel.

## I. INTRODUCTION

**F**AULT detection and isolation is a potentially powerful tool for achieving security and effective maintenance in various types of processes. Applications in aviation and automotive technology are common (see, for example, [2]), but there are also many examples of fault detection in general industrial processes, like electrical motors and hydraulic systems [3], [4]. See [5] for a survey of recent simulations and implementations of fault detection systems.

The basic terminology and techniques for fault detection can be found in the survey by Frank [6]. State estimation by observers is often used. A number of different techniques exist, for example unknown input observers, dedicated observers, parity space, and Kalman filter methods. A survey on nonlinear observers is given in [7]. Fault detection in nonlinear systems is, for example, treated in [8] and [9].

The fundamental question in fault detection is whether the nominal nonfaulty model should be accepted or rejected. This fact emphasizes the similarities to model validation. The detection of abrupt and incipient faults can thus be interpreted as local and global model validation, respectively.

This article concerns the detection of incipient faults (leakages) in the valves of a pressurized coal injection vessel in a blast furnace process. The blast furnace is used in iron making to reduce ore into hot metal. The reduction agent is coal, in the form of coke or coal powder, of which the latter is less expensive. Coal powder can also be easier used to control the temperature of the blast furnace. The prime drawback of coal powder is its inflammability. The ability to self-ignite in contact with air makes it inconvenient to transport. Any storage and transport has to take place under inert conditions and it has to be injected under pressure directly into the reaction core. For these reasons, it is of interest to have a reliable coal powder injection plant. A leakage in a valve could for example make it possible for air to enter the injection vessel with probably catastrophic consequences. In fact, one of the prime motivations for this work was a fire in one of the injection vessels at SSAB Tunplåt in Luleå, Sweden.

This paper is organized as follows. The rest of Section I is devoted to a brief description of the plant. In Section II, models of the plant are derived. The models are physically motivated with unknown coefficients that are estimated from logged data. Models for the expected behavior of different leakages in the time domain are also developed. Sections III and IV deal with fault detection and isolation, respectively. Fault detection observers are developed and the generalized

Manuscript received September 2, 1997; revised August 18, 1998. Recommended by Associate Editor, R. Takahashi. This work was supported by *Norrbottnens Forskningsråd*. An abridged version of this article was presented at the 1998 American Control Conference, Philadelphia, PA.

The authors are with the Luleå University of Technology, S-971 87 Luleå, Sweden.

Publisher Item Identifier S 1063-6536(99)09044-2.

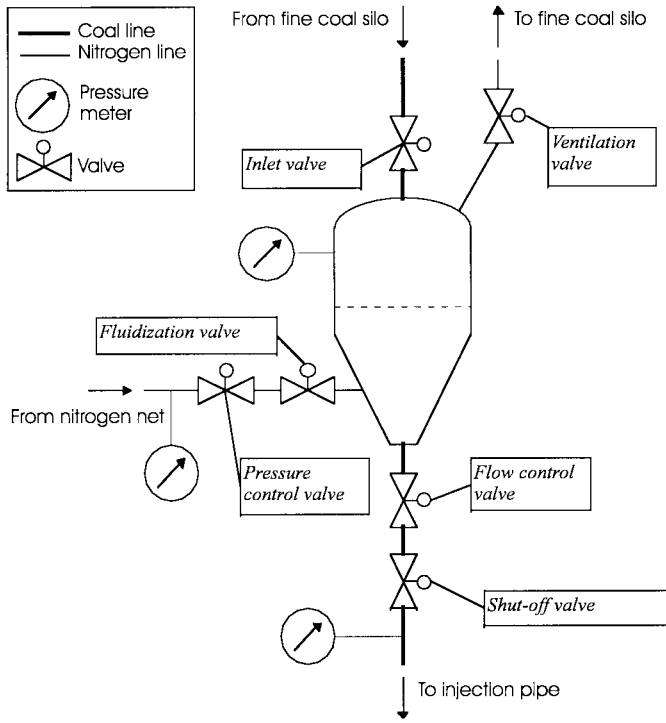


Fig. 1. The injection vessel.

likelihood ratio is used to determine if and where a leakage has occurred. Section V shows the results from experiments in the plant and Section VI gives the conclusions.

#### A. The Plant

An overview of an injection vessel is shown in Fig. 1. In addition to the sensors in the figure, there is also a weighing equipment that measures the total mass of the content in the injection vessel. The injection process is cyclic and can be divided into the four phases shown in Table I.

## II. MODELING

#### A. Output Transformation

The pressure and total mass ( $p$  and  $m$ ) of the vessel can be calculated from the masses of coal and nitrogen ( $m_C$  and  $m_N$ ) using basic physical principles including the ideal gas law. With the definitions  $y \triangleq [m \ p]^T$  and  $x \triangleq [m_C \ m_N]^T$  the transformation can be expressed as

$$y = h(x) \triangleq \begin{bmatrix} m_C + m_N \\ m_N \frac{R_N T \rho_C}{V \rho_C - m_C} \end{bmatrix}.$$

Index  $C$  in the equation above refers to pure coal and not coal powder. The reason for this is that the nitrogen is assumed to fill out the space between the coal particles. Since  $h(x)$  is invertible, the coal and nitrogen masses can be considered measurable. The inverse transformation is given below

$$x = h^{-1}(y) = \begin{bmatrix} \frac{m R_N T \rho_C - p V \rho_C}{R_N T \rho_C - p} \\ \frac{V \rho_C - m}{p \frac{R_N T \rho_C - p}{m R_N T \rho_C - p}} \end{bmatrix}.$$

Upon entering the vessel, the nitrogen passes through the coal powder. Since nitrogen has much lower heat capacity than coal powder it is assumed to be momentarily heated to the temperature of the coal powder (60–70°C). Therefore  $T$  is given the constant value of 338K.

#### B. Flow through Valves

Expressions for mass flow of fluids through restrictions can be derived from Bernoulli's law. For an incompressible liquid the flow is

$$q(p_1, p_2) = a f_{liq}(p_1, p_2) \triangleq a \sqrt{2\rho(p_1 - p_2)} \quad (1)$$

where  $p_1$  is the pressure on the inlet side of the restriction and  $p_2$  is the pressure on the opposite side. The constant  $\rho$  denotes the density of the liquid and  $a$  is the minimum cross-section area of the flow.

The major difference between a liquid and a gas is the compressibility of the latter. If the dynamic effects due to this property are neglected and the expansion process in the valve is assumed to be adiabatic, then the following expression holds for the mass flow of an ideal gas as shown in (2) at the bottom of the page.

The constant  $R$  and  $\gamma$  are the molecular mass and the compressibility factor of the gas, respectively, while  $T_1$  represents the temperature on the inlet side.

For a control valve, the area  $a$  in (1) and (2) is a function of the input signal  $u$ , i.e.,  $a = kg(u(t))$  where  $k$  is a scaling factor and  $g(u)$  is called the characteristic function of the valve. In order to make the definition above unambiguous it is also stated that  $g(1) = 1$ .

A common characteristic function is the "equal percentage" [10]. For a valve with such characteristic, a certain increase in the control signal gives an increase in the flow that is proportional to the flow. This leads to an exponential function. Since an exponential function is always positive, a deadzone  $d$  has to be included in the characteristic function

$$g(u) = g_{\text{exp}}(u, c, d) \triangleq \begin{cases} e^{c(u-1)}, & u > d \\ 0, & \text{otherwise.} \end{cases} \quad (3)$$

$$q(p_1, p_2) = a f_{\text{gas}}(p_1, p_2) \triangleq a p_1 \begin{cases} \left(\frac{p_2}{p_1}\right)^{1/\gamma} \sqrt{\frac{2\gamma}{RT_1(\gamma-1)} \left[1 - \left(\frac{p_2}{p_1}\right)^{(\gamma-1)/\gamma}\right]}, & \frac{p_2}{p_1} < \left(\frac{2}{\gamma+1}\right)^{\gamma/(\gamma-1)} \\ \left(\frac{2}{\gamma+1}\right)^{1/(\gamma-1)} \sqrt{\frac{2\gamma}{RT_1(\gamma+1)}}, & \text{otherwise.} \end{cases} \quad (2)$$

TABLE I  
THE INJECTION CYCLE

Phase	Action	Effect
Charging	Inlet valve is opened	The vessel is filled with coal powder
Pressurization	Inlet and ventilation valves are closed. Fluidization and pressure control valves are opened	The pressure rises to 950 kPa
Injection	Flow control and shut-off valves are opened	Coal powder is injected into the blast furnace
Ventilation	Ventilation valve is opened. All other valves are closed	The vessel is depressurized

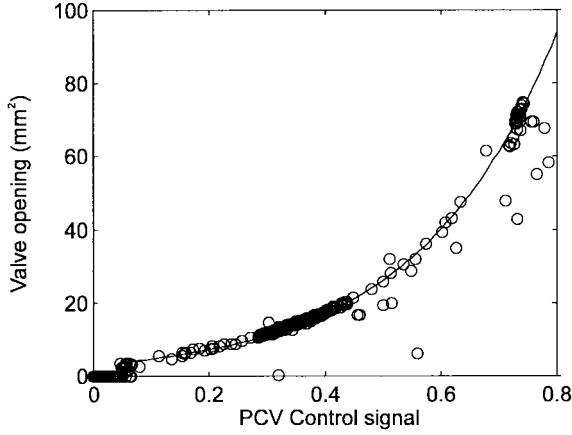


Fig. 2. Characteristic function of the PCV.

### C. The Valves of the Process

1) *The Pressure Control Valve (PCV)*: The flow of nitrogen through the PCV can be expressed as

$$q_{N,P} = k_{N,P} f_{\text{gas}}(p_N, p) g_P(u_P) \quad (4)$$

where  $p_N$  is the pressure in the nitrogen net and  $u_P$  is the input signal to the PCV, while  $g_P$  is the characteristic function of the PCV.

Since the nitrogen flow  $q_{N,P}$  is measured by a flow meter, only the characteristic function  $g_P$  and the factor  $k_{N,P}$  in (4) are unknown. These unknown factors can be isolated to give

$$k_{N,P} g_P(u_P) = \frac{q_{N,P}}{f_{\text{gas}}(p_N, p)}. \quad (5)$$

Fig. 2 shows the right side of (5) (circles) for one pressurization and injection. Since  $k_{N,P}$  is constant, the circles also represent the scaled characteristic function. It is obvious that the characteristic function is exponential, i.e., of the type “equal percentage” (3), thus  $g_P(u_P) = g_{\text{exp}}(u_P, c_P, d_P)$ . An approximate value of the deadzone  $d_P$  ( $\approx 5\%$ ) can also be obtained from the figure. If the deadzone is excluded, the logarithm of (5) is linear in the parameters  $c_P$  and  $\ln(k_{N,P})$ . These parameters can thus be produced by least-squares identification. Note that it is possible to show that a scale error in the flow meter will only affect the estimate of  $k_{N,P}$  and not of  $c_P$ . The value of  $k_{N,P}$  will be estimated more accurately later. The identified characteristic function is also shown in Fig. 2.

2) *The Flow Control Valve (FCV)*: Through the FCV, there is a flow of both nitrogen and coal powder, i.e., a two component flow. To simplify the model, the two flows are assumed to be independent, and the coal powder is regarded as a liquid. More accurate models are available [11], but since the flow of coal powder is controlled and to be held constant, the accuracy in this aspect of the physical model is not of crucial importance. If the flow is characterized by small variations around an equilibrium point, then the nonlinear plant behaves like a linear system around this point. A certain approximation of the unmodeled behavior will thus be included in the identified model.

The flow of coal powder is  $q_{C,F} = k_{C,F} f_{\text{liq}}(p, p_I) g_F(u_F)$  where  $p_I$  is the pressure in the injection pipe,  $u_F$  is the control signal for the FCV, and  $g_F$  is the characteristic function of the FCV. The nitrogen flow is  $q_{N,F} = k_{N,F} f_{\text{gas}}(p, p_I) g_F(u_F)$ .

In drawings of the FCV, it can be seen that it has a deadzone,  $d_F$ , of  $\approx 21\%$ . Apart from this, the characteristic function is assumed to be linear

$$g_F(u_F) = \begin{cases} \frac{1}{1-d_F} (u_F - d_F), & u_F > d_F \\ 0, & \text{otherwise.} \end{cases}$$

3) *The Ventilation Valve (VV)*: In order to obtain a smooth flow in the ventilation valve, it is controlled by a hydraulic feedback. Since this control signal is not measured, the VV has to be modeled as a closed loop.

The flow through the VV goes to the fine coal silo, which is assumed to have constant pressure, and is thus a function of the pressure in the injection vessel only, i.e.,  $q_{N,V} = f_{N,V}(p)$ . The function  $f_{N,V}(p)$  is simply taken to be a polynomial of order  $J$ , thus  $f_{N,V}(p) = \sum_{j=0}^J k_j p^j$ .

### D. Leakages

Three different leakages are considered (Table II). The set of leakages is defined as  $\mathcal{L} \triangleq \{\mathcal{A}, \mathcal{N}, \mathcal{I}, \emptyset\}$ . A leakage can be looked upon as the flow through a valve with an unknown control signal. The nitrogen leakage flow can thus be represented by

$$q_\ell = k_\ell f_\ell(\cdot) \quad \ell \in \mathcal{L} \quad (6)$$

where  $k_\ell$  is an unknown time-varying factor and  $f_\ell(\cdot)$  is a function of the pressures on each side of the leakage. The

TABLE II  
LEAKAGES

Leakage	Notation
To the atmosphere	$\mathcal{A}$
From the nitrogen net	$\mathcal{N}$
To/from the injection pipe	$\mathcal{I}$
No Leakage	$\emptyset$

trivial leakage function for “no leakage” is  $f_\emptyset = 0$ . The other leakage functions are  $f_{\mathcal{A}}(p, p_{\mathcal{A}}) = f_{\text{gas}}(p, p_{\mathcal{A}})$ ,  $f_{\mathcal{N}}(p_{\mathcal{N}}, p) = f_{\text{gas}}(p_{\mathcal{N}}, p)$ , and  $f_{\mathcal{I}}(p, p_{\mathcal{I}}) = \text{sign}(p - p_{\mathcal{I}})f_{\text{gas}}(\max(p, p_{\mathcal{I}}), \min(p, p_{\mathcal{I}}))$ . The last equation is due to the fact that the pressure in the vessel can be higher as well as lower than the pressure in the injection pipe and thus the leakage flow can take place in both directions.

### E. Entire System

1) *Pressurization and Injection*: During the pressurization and injection phases the material transport takes place through the PCV and the FCV. Therefore, the change in the coal and nitrogen masses of the vessel can be expressed as

$$\begin{aligned} \dot{m}_C &= -q_{C,F} \\ \dot{m}_N &= -q_{N,F} + q_{N,P}. \end{aligned} \quad (7)$$

The transformed input signal is defined

$$u(v, w, y) \triangleq \begin{bmatrix} u_{C,F} \\ u_{N,F} \\ u_{N,P} \end{bmatrix} \triangleq \begin{bmatrix} f_{\text{liq}}(p, p_{\mathcal{I}})g_F(u_F) \\ f_{\text{gas}}(p, p_{\mathcal{I}})g_F(u_F) \\ f_{\text{gas}}(p_{\mathcal{N}}, p)g_P(u_P) \end{bmatrix}$$

where  $v \triangleq [u_F \quad u_P]^T$  is the real input signal and  $w \triangleq [p_{\mathcal{I}} \quad p_{\mathcal{N}}]^T$  represents the measurable disturbances. Thus, the process model for pressurization and injection can be written as

$$\begin{aligned} \dot{x} &= Ax + Bu(v, w, y) \\ y &= h(x) \end{aligned} \quad (8)$$

where

$$A \triangleq \begin{bmatrix} a_C & 0 \\ 0 & a_N \end{bmatrix} \quad B \triangleq \begin{bmatrix} k_{C,F} & 0 & 0 \\ 0 & -k_{N,F} & k_{N,P} \end{bmatrix}.$$

In principle, the variables  $a_C$  and  $a_N$  should be equal to zero. But, in order to obtain extra degrees of freedom, they are considered to be unknown. When identifying, the parameter  $a_N$  always takes a small negative value, which probably suggests inherent leakage in the vessel. The other parameter,  $a_C$  takes on a small positive value, i.e., introducing an unstable mode. However, since this instability is very small and not physically motivated, it does not present any problem.

Figs. 3 and 4 show a simulation of the entire nonlinear system with input signals  $u_F$  and  $u_P$  and output signals  $p$  and  $m$ .

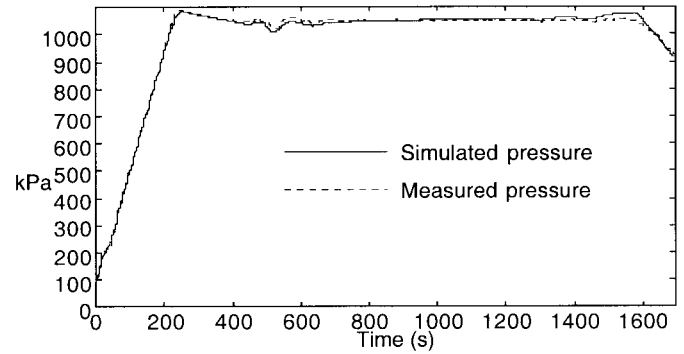


Fig. 3. Simulation of the pressure in the vessel during pressurization and injection.

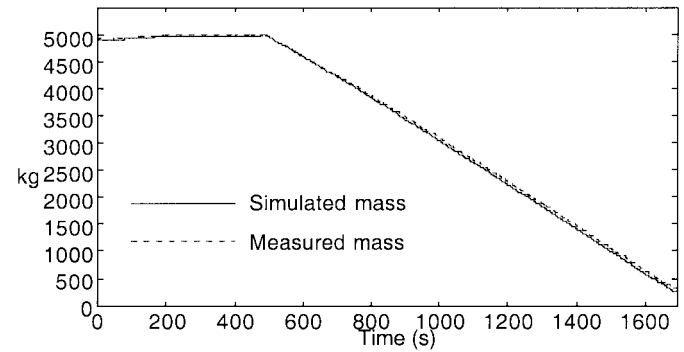


Fig. 4. Simulation of the mass in the vessel during pressurization and injection.

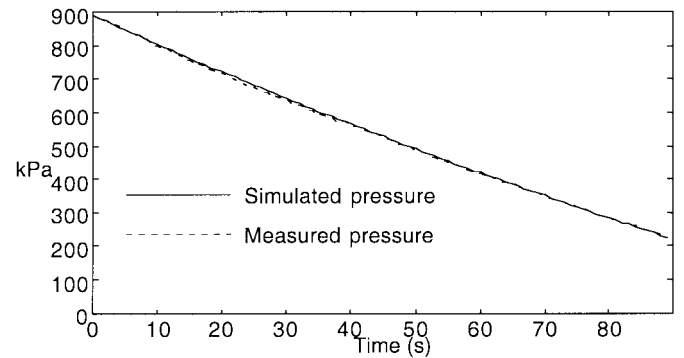


Fig. 5. Simulation of the pressure in the vessel during ventilation.

2) *Ventilation*: During the ventilation phase, the only material flow is the nitrogen flow through the ventilation valve. Therefore

$$\begin{aligned} \dot{m}_C &= 0 \\ \dot{m}_N &= -q_{N,V} = -f_{N,V}(p). \end{aligned} \quad (9)$$

The nitrogen flow can be accurately described by a first-order polynomial. This means that (9) can be written as

$$\dot{m}_N = -k_0 - k_1 c(m_C) m_N \quad (10)$$

where  $c(m_C) \triangleq R_N T \rho_C / (V \rho_C - m_C)$ . The coefficients  $k_0$  and  $k_1$  have been produced by least squares identification. Fig. 5 shows a simulation of the pressure during ventilation.

### III. FAULT DETECTION

The leakage flow is modeled as an extra term added to the right hand side of (7) and (9). The purpose of the fault detection algorithm is thus to calculate this term. However, the presence of noise makes it necessary to utilize filtering. A properly designed observer should be able to distinguish between the slow dynamics of the process and the relatively fast dynamics of the disturbances.

The nonlinear models developed in the previous section are of the Hammerstein type and thus linear observers can be used.

#### A. Pressurization and Injection

When leakage is taken into account, (7) has to be extended with the term  $q_L$ , that represents the net leakage of nitrogen into the vessel, thus  $\dot{m}_N = -q_{N,F} + q_{N,P} + q_L$ . An observer for the system (8) is given by

$$\dot{\hat{x}} = A\hat{x} + Bu(v, w, \hat{y}) + K\epsilon \quad (11)$$

$$\hat{y} = h(\hat{x}) \quad (12)$$

where

$$\begin{aligned} \epsilon &\triangleq [\epsilon_C \quad \epsilon_N]^T \triangleq [m_C - \hat{m}_C \quad m_N - \hat{m}_N]^T \\ &= h^{-1}(y) - \hat{x}. \end{aligned}$$

Since in this system the state variables are decoupled (i.e.,  $A$  is diagonal), it is assumed that a diagonal observer gain matrix is sufficient

$$K \triangleq \begin{bmatrix} K_C & 0 \\ 0 & K_N \end{bmatrix}. \quad (13)$$

Note, however, that when calculating the transformed input signal,  $u$ , the estimated state  $\hat{x}$  is used, thus introducing a dependence between the state variables, and therefore the full-order observer is used. A full-order observer also has a greater robustness to modeling errors (see Appendix A).

With the definitions above, it can be shown that the residual  $\epsilon_N$  is the net leakage  $q_L$ , filtered through a first-order filter. This filter is given by

$$\epsilon_N(t) = \frac{1}{\mathbf{p} - a_N + K_N} q_L(t) = H_{\mathfrak{F}}(\mathbf{p})q_L(t)$$

where  $\mathbf{p}$  is the differentiation operator. If the net leakage is assumed to be slowly varying in time, the residual divided with the static gain of the filter above is a good approximation of the net leakage corrupted by white noise.

$$\hat{q}_L(t) = \frac{1}{H_{\mathfrak{F}}(0)} \epsilon_N(t). \quad (14)$$

#### B. Ventilation

The net leakage  $q_L$  is introduced in the ventilation system in a manner similar to the leakage in the pressurization and injection system, i.e.,  $\dot{m}_N = -q_{N,V} + q_L$ . An observer for the ventilation phase process (10) is given by  $\dot{\hat{m}}_N = -k_0 - k_1 c(m_C) \hat{m}_N + K_N \epsilon_N$ . The residual  $\epsilon_N$  is then the net leakage filtered through a first-order filter

$$\epsilon_N(t) = \frac{1}{\mathbf{p} + k_1 c(m_C) + K_N} q_L(t) = H_{\mathfrak{V}}(\mathbf{p})q_L(t).$$

As before, the residual is divided with the static gain of the filter

$$\hat{q}_L(t) = \frac{1}{H_{\mathfrak{V}}(0)} \epsilon_N(t). \quad (15)$$

### IV. ISOLATION OF LEAKAGES

The development of the models and the observers in the previous sections is performed in continuous time to facilitate physical interpretation. However, since the systems are of the Hammerstein type, it is a straightforward task to discretize the observers. In the following, all signals are assumed to be discrete, which is indicated by the new time-variable  $n$ .

The calculated leakage is assumed to be the sum of a scaled leakage function and a disturbance, i.e.,  $\hat{q}_L(n) = k_\ell f_\ell(n) + e(n)$  where  $\ell \in \mathcal{L}$  and the term  $e(n)$  is stationary zero-mean white Gaussian noise with variance  $\sigma^2$ , i.e.,  $e(n) \in \mathcal{N}(0, \sigma)$ .

Actually,  $e(n)$  is not Gaussian (probably due to unmodeled nonlinearities), but this fact does not have any major influence on the results. When the transient behavior is excluded from the data, the residual is fairly near normal distribution, but the results are virtually the same.

The factor  $k_\ell$  in (6) represents the size of the hole through which the leakage flow takes place. This means that  $k_\ell$  varies slowly in time when considering incipient leakages. If it is assumed to be constant during a reasonably long period of time (for example a process cycle), it can be estimated using the generalized likelihood ratio.

#### A. Leakage Hypothesis Testing

To isolate the leakage flow  $\hat{q}_L(t)$  to a certain valve or place, an automatic method is necessary. It is also desirable to provide the user with an estimate of the physical size of the leakage and the confidence level of its detection and isolation. This motivates the use of the generalized likelihood ratio (GLR) [12] for fault isolation.

Four hypotheses ( $\mathcal{H}_\emptyset$ ,  $\mathcal{H}_A$ ,  $\mathcal{H}_N$ , and  $\mathcal{H}_T$ ) are formed in agreement with the leakage events. The three leakage hypotheses are tested one by one against  $\mathcal{H}_\emptyset$  using the GLR. If  $\mathcal{H}_\emptyset$  is rejected in more than one of these tests, the hypothesis with the highest GLR is accepted. The likelihood functions for the hypotheses can be expressed as

$$P_\ell(\hat{q}_L) = \prod_{n=1}^N \frac{1}{\sigma} \varphi\left(\frac{\hat{q}_L(n) - k_\ell f_\ell(n)}{\sigma}\right)$$

where  $\varphi(\cdot) = (1/\sqrt{2\pi}) e^{-(\cdot)^2/2}$ .

The GLR for each leakage hypothesis is

$$\Lambda_\ell(\hat{q}_L) = \frac{\sup_{k_\ell > 0} P_\ell(\hat{q}_L)}{P_\emptyset(\hat{q}_L)}.$$

The restriction on  $k_\ell$  comes from the fact that a negative  $k_\ell$  would imply a leakage flow from a lower pressure to a higher.

It can be shown that under the conditions above, the leakage likelihood function,  $P_\ell(\hat{q}_L)$ , is maximized by

$$\hat{k}_\ell = \arg \sup_{k_\ell > 0} P_\ell(\hat{q}_L) = \begin{cases} \frac{C_\ell}{\sum_{n=1}^N f_\ell^2(n)}, & C_\ell > 0 \\ 0, & \text{otherwise} \end{cases}$$

where  $C_\ell \triangleq \sum_{n=1}^N \hat{q}_L(n) f_\ell(n)$ .

TABLE III  
THE MEANS OF EMULATING LEAKAGES

Leakage	Experimental means
To atmosphere	Opening a safety valve slightly
From the nitrogen net	Opening the fluidization- and pressure control valves partly
To/from the injection pipe	No experiment due to safety reasons

The logarithmic GLR can then be expressed as

$$\ln(\Lambda_\ell(\hat{q}_L)) = \begin{cases} \frac{C_\ell^2}{2\sigma^2 \sum_{n=1}^N f_\ell^2(n)}, & C_\ell > 0 \\ 0, & \text{otherwise.} \end{cases}$$

A threshold value,  $\lambda$ , for  $\Lambda_\ell$  must be set. If  $\Lambda_\ell$  exceeds this value then the null hypothesis,  $\mathcal{H}_0$ , is rejected. The threshold is generally calculated using the probability of rejecting the null hypothesis when it is true, i.e.,  $\mathbb{P}[\Lambda_\ell(\hat{q}_L) > \lambda] \triangleq \alpha$  where  $\mathbb{P}$  is the probability operator. The probability  $\alpha$  is called the level of the test and is usually set to a value in the range of  $0.1\% \leq \alpha \leq 5\%$ . In the case of the pressurization and injection system, however, the severity of the modeling errors causes the assumptions of stationarity and zero-mean conditions of the disturbance  $e(n)$  to fall. This makes it necessary to use very low levels to prevent a high rate of false alarms. For this reason, no test level is chosen but instead the threshold  $\lambda$  is chosen on the basis of experimental data (Section V).

## V. PRACTICAL RESULTS

In order to validate the methods developed in this paper, experiments on the plant were carried out. Different leakages were created during a period of six process cycles. The means of creating the leakages are shown in Table III.

The relevant signals were logged with a sampling time of 1 s and the net leakage was then calculated using (14) and (15). The logarithmic GLR,  $\ln(\Lambda_\ell(\hat{q}_L))$ , for each leakage type and each cycle is shown as diagrams in Figs. 6 and 7. The dashed line in Fig. 7 shows the threshold for GLR when  $\alpha = 1\%$  while the two dashed lines in Fig. 6 mark an interval for the threshold. Note that the hypothesis of leakage from the nitrogen net is absent in Fig. 6, since the pressure control valve, which connects the nitrogen net with the vessel, is open during pressurization and injection. There can, for obvious reasons, not be a leakage in an open valve.

Table IV shows the conclusions that are drawn for the pressurization and injection phases when the threshold for the GLR is placed anywhere between the dashed lines of Fig. 6. Table V shows the conclusions for the ventilation phase with level 1%. Included in the tables are also the real leakages. It can be seen that the right conclusions are drawn in all cases but one. In this case there were two simultaneous leakages (atmosphere and nitrogen net) that nearly cancelled each other.

## VI. CONCLUSIONS

It has been shown that model-based fault detection is a possible way of detecting leakages in the valves of a

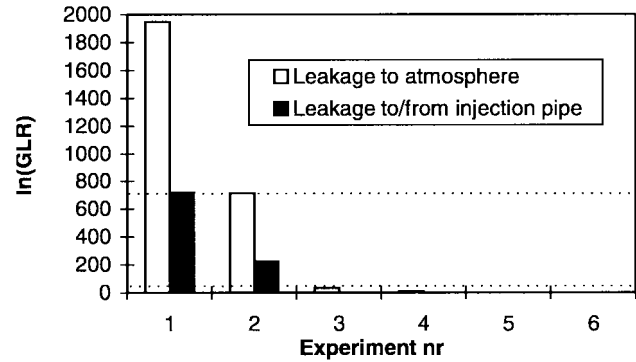


Fig. 6. The logarithm of the GLR for each leakage type and each experiment during pressurization and injection.

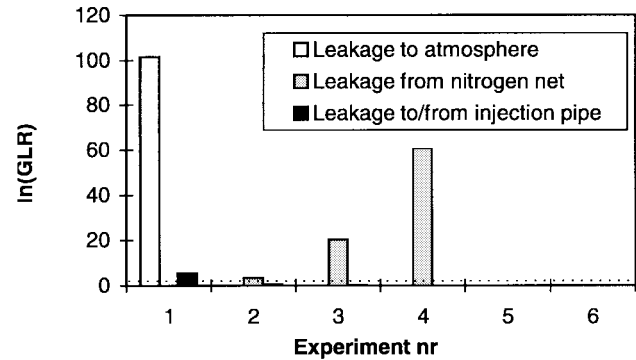


Fig. 7. The logarithm of the GLR for each leakage type and each experiment during ventilation.

TABLE IV  
THE LEAKAGES DURING PRESSURIZATION AND INJECTION

Cycle	Conclusion	Real Leakage
1	Atmosphere	Atmosphere
2	Atmosphere	Atmosphere
3	No leakage	No leakage
4	No leakage	No leakage
5	No leakage	No leakage
6	No leakage	No leakage

pressurized system. A grey-box model for an injection vessel is developed and a method for detecting and isolating leakages is suggested. Experiments with leakages in different valves of the plant showed the effectiveness of the method.

## APPENDIX A SENSITIVITY ANALYSIS

The close connection between observer order and robustness is well known [13]. In this particular application, how-

TABLE V  
THE LEAKAGES DURING VENTILATION

Cycle	Conclusion	Real Leakage
1	Atmosphere	Atmosphere
2	Nitrogen net	Atmosphere and nitrogen net
3	Nitrogen net	Nitrogen net
4	Nitrogen net	Nitrogen net
5	No leakage	No leakage
6	No leakage	No leakage

ever, a closer study has been made due to the nonlinear plant.

The process model for the injection phase can be linearized around a working point giving

$$\dot{x} = A_{\text{lin}}x + B_{\text{lin}}v + Dq_L + \Delta A_{\text{lin}}x + \Delta B_{\text{lin}}v. \quad (16)$$

where  $D \triangleq [0 \ 1]^T$ . Furthermore

$$A_{\text{lin}} \triangleq \begin{bmatrix} A_C \\ A_N \end{bmatrix} \triangleq \begin{bmatrix} A_{CC} & A_{NC} \\ A_{CN} & A_{NN} \end{bmatrix}$$

$$B_{\text{lin}} \triangleq \begin{bmatrix} B_C \\ B_N \end{bmatrix} \triangleq \begin{bmatrix} B_{CC} & B_{NC} \\ B_{CN} & B_{NN} \end{bmatrix}$$

while  $\Delta A_{\text{lin}}$  and  $\Delta B_{\text{lin}}$  represent the uncertainties of  $A_{\text{lin}}$  and  $B_{\text{lin}}$ . The explicit equations for calculating the elements of  $A_{\text{lin}}$  and  $B_{\text{lin}}$  are not shown here in order to save space. Important to note, however, is that both off-diagonal elements of  $A_{\text{lin}}$  are nonzero. An identified model of the injection vessel during the injection phase also exists [14], which is very close to the linearized model.

The fault detection observer can, in the same manner, be linearized to

$$\dot{\hat{x}} = A_{\text{lin}}\hat{x} + B_{\text{lin}}v + K(x - \hat{x}) \quad (17)$$

where  $K$  is defined according to (13). The residual of the linearized observer can be expressed as

$$\epsilon = G(\mathbf{p})(Dq_L + \Delta A_{\text{lin}}x + \Delta B_{\text{lin}}v)$$

where

$$G(\mathbf{p}) \triangleq (\mathbf{p}I - A_{\text{lin}} + K)^{-1}.$$

Since the off-diagonal elements of  $A_{\text{lin}}$  are very small, and thus (16) is nearly decoupled, it might be argued that a reduced order observer should be used instead. The reduced order linearized process model and the corresponding observer are then

$$\dot{m}_N = A_{NN}m_N + B_Nv + q_L + \Delta A_Nx + \Delta B_Nv$$

$$\dot{\hat{m}}_N = A_{NN}\hat{m}_N + B_Nv + K_1(m_N - \hat{m}_N) \quad (18)$$

where  $\Delta A_N$  and  $\Delta B_N$  are the uncertainties of  $A_N$  and  $B_N$ . The error process for the linearized reduced order system is thus

$$\epsilon_1 = G_1(\mathbf{p})(Dq_L + \Delta A_Nx + \Delta B_Nv)$$

where

$$G_1(\mathbf{p}) = \frac{1}{\mathbf{p} - A_{NN} + K_1}.$$

If the input signal  $v$  is kept at the constant level  $v_0$ , then the sensitivity of  $\epsilon_1$  to parameter errors in  $B_N$ ,  $\partial\epsilon_1/\partial B_N$  can be calculated from the equation above. Corresponding sensitivities can be determined for  $A_N$  and the leakage  $q_L$ . All these sensitivities will only differ by constant factors from

$$S_1(\mathbf{p}) \triangleq G_1(\mathbf{p}).$$

The sensitivity of  $\epsilon_N$  to the same parameters for the full-order observer is

$$S(\mathbf{p}) = [0 \ 1]G(\mathbf{p})[0 \ 1]^T.$$

Since incipient leakages are considered, it is desirable to have high sensitivity to low frequencies and low sensitivity to higher frequencies to reduce the impact of parameter variations. It will be shown below that even with the diagonal feedback gain matrix  $K$ , this can always be done better with the full-order observer (17) than with the reduced-order observer (18), provided that  $A_{\text{lin}}$  does not have zeros off the diagonal. If a general feedback gain  $K$  is used, even better results can be accomplished, but this has not been investigated any further.

*Proposition 1:* Let  $A_{\text{lin}}$  be defined as above and let both off-diagonal elements of  $A_{\text{lin}}$  be nonzero. Then, for any  $\omega_0 > 0$  and  $K_1 \neq A_{NN}$ , there exists a real diagonal  $K$  such that  $S(\mathbf{p})$  is asymptotically stable and

$$\begin{cases} |S(j\omega)| > |S_1(j\omega)| & 0 < \omega < \omega_0 \\ |S(j\omega)| < |S_1(j\omega)| & \omega > \omega_0. \end{cases} \quad (19)$$

*Proof:* Define the variables  $a_{11} \triangleq A_{CC} - K_C$  and  $a_{22} \triangleq A_{NN} - K_N$  and the nonzero constants  $a_1 \triangleq A_{NN} - K_1$  and  $b \triangleq A_{NC}A_{CN}$ . Then the sensitivity functions can be expressed as

$$S_1(\mathbf{p}) = \frac{1}{\mathbf{p} - a_1}$$

$$S(\mathbf{p}) = \frac{\mathbf{p} - a_{11}}{\mathbf{p}^2 - \mathbf{p}(a_{11} + a_{22}) + a_{11}a_{22} - b}.$$

The conditions for asymptotic stability of  $S(\mathbf{p})$  are

$$a_{11} + a_{22} < 0 \quad (20)$$

$$a_{11}a_{22} - b > 0 \quad (21)$$

and the squared absolute values of the sensitivity functions are

$$|S_1(j\omega)|^2 = \frac{1}{\omega^2 + a_1^2}$$

$$|S(j\omega)|^2 = \frac{\omega^2 + a_{11}^2}{(a_{11}a_{22} - b - \omega^2)^2 + \omega^2(a_{11} + a_{22})^2}.$$

Straightforward calculations yield that (19) is equivalent to

$$\phi(\omega) < 0, \quad 0 < \omega < \omega_0$$

$$\phi(\omega) > 0, \quad \omega > \omega_0$$

where

$$\phi(\omega) \triangleq \omega^2(a_{22}^2 - a_1^2 + 2b) - a_1^2a_{11}^2 + (a_{11}a_{22} - b)^2.$$

This is true if and only if

$$\phi(\omega_0) = 0 \quad (22)$$

$$a_{22}^2 - a_1^2 + 2b > 0. \quad (23)$$

Note that if  $a_{11} \rightarrow -a_{11}$  and  $a_{22} \rightarrow -a_{22}$  then the left-hand side of (20) changes sign while (21)–(23) remain intact and thus condition (20) can be replaced by

$$a_{11} + a_{22} \neq 0. \quad (24)$$

Define  $\zeta \triangleq a_{11}a_{22} - b$  and  $\xi \triangleq a_{22}^2 - a_1^2 + 2b$ . The condition  $a_{22}^2 > 0$ , which is equivalent to

$$\xi > 2b - a_1^2 \quad (25)$$

guarantees that  $a_{11}$  and  $a_{22}$  are real and finite. The definitions of  $\zeta$  and  $\xi$  imply that  $a_{11} = (\zeta + b)/a_{22}$  and  $a_{22}^2 = \xi + a_1^2 - 2b$ , which, when substituted into (21)–(24), while combining (23) and (25), yields

$$\begin{cases} F(\zeta, \xi) = 0 \\ \zeta > 0 \\ \xi > \Xi_0 \\ \xi \neq \ell_1(\zeta) \end{cases} \quad (26)$$

where

$$\begin{aligned} F(\zeta, \xi) &\triangleq \zeta^2(\xi - 2b) - 2\zeta ba_1^2 + \xi^2\omega_0^2 \\ &\quad + \xi\omega_0^2(a_1^2 - 2b) - b^2a_1^2 \\ \Xi_0 &\triangleq \max(0, 2b - a_1^2) \\ \ell_1(\zeta) &\triangleq -\zeta + b - a_1^2. \end{aligned}$$

Define the line  $\xi = \ell_2(\zeta) \triangleq k\zeta + \Xi_1$ , where  $k > 0$  and  $\Xi_1 \triangleq \max(\Xi_0, b - a_1^2)$ . Obviously,  $\zeta > 0$  implies that  $\xi > \Xi_0$  on this line, since  $\Xi_1 \geq \Xi_0$ . It is also clear that  $\ell_1$  and  $\ell_2$  do not intersect for  $\zeta > 0$ .

Substitution of  $\xi = \ell_2(\zeta)$  into  $F(\zeta, \xi)$  yields

$$\begin{aligned} f(\zeta) &= k\zeta^3 + \zeta^2(k^2\omega_0^2 + \Xi_1 - 2b) \\ &\quad + \zeta(k\omega_0^2(2\Xi_1 + a_1^2 - 2b) - 2a_1^2b) \\ &\quad + \Xi_1\omega_0^2(\Xi_1 + a_1^2 - 2b) - a_1^2b^2. \end{aligned}$$

The constant  $\Xi_1$  can take on the values zero,  $2b - a_1^2$ , or  $b - a_1^2$ . If  $\Xi_1 = 0$  or  $\Xi_1 = 2b - a_1^2$  then  $f(0) = -a_1^2b^2 < 0$ . If, on the other hand,  $\Xi_1 = b - a_1^2$  then  $f(0) = -3b\omega_0^2(b - a_1^2) - a_1^2b^2$ . In this case, due to the definition of  $\Xi_1$  and  $\Xi_0$ , it follows that  $b - a_1^2 > 0$ , which implies that  $b > 0$  and thus  $f(0) < 0$ . Note also that there exists a  $Z > 0$  such that  $f(Z) > 0$  due to the cubic term of  $f(\zeta)$ .

Since  $f(0) < 0$ ,  $f(Z) > 0$ , and  $f(\zeta)$  is continuous, there must exist a  $\zeta_0 \in ]0, Z[$  such that  $f(\zeta_0) = 0$ , and thus  $F(\zeta_0, \ell_2(\zeta_0)) = 0$ . All the conditions of (26) are thereby satisfied and the proposition follows. Q.E.D.

#### ACKNOWLEDGMENT

The authors would like to thank the personnel of SSAB Tunnpilat in Luleå and in particular R. Johansson, I. Lundström, and B. Paavola for their time and effort.

#### REFERENCES

- [1] A. Johansson and A. Medvedev, "Model-based leakage detection in a pulverized coal injection vessel," in *Proc. 1998 Amer. Contr. Conf.*, 1998, vol. 3, pp. 1742–1746.
- [2] F. Gustafsson, "Slip-based tire-road friction estimation," *Automatica*, vol. 33, no. 6, pp. 1087–1099, 1997.
- [3] J. Chai, R. Lyon, and J. Lang, "Noninvasive diagnostics of motor-operated valves," in *Proc. Amer. Contr. Conf.*, 1997, vol. 2, pp. 2006–2012.
- [4] W. Ge and C.-Z. Fang, "Detection of faulty components via robust observation," *Int. J. Contr.*, vol. 47, no. 6, pp. 581–599, 1988.
- [5] R. Isermann and P. Ballé, "Trends in the application of model-based fault detection and diagnosis of technical processes," in *IFAC World Congr. Proc.*, 1996, CD-ROM.
- [6] P. M. Frank, "Fault diagnosis in dynamic systems using analytical and knowledge-based redundancy—A survey and some new results," *Automatica*, vol. 26, no. 3, pp. 459–474, 1990.
- [7] E. A. Misawa and J. K. Hedrick, "Nonlinear observers—A state-of-the-art survey," *J. Dynamic Syst., Measurement, Contr.*, vol. 111, pp. 344–352, Sept. 1989.
- [8] J. Wünnenberg and P. M. Frank, "Dynamic model-based incipient fault detection concepts for robots," in *11th IFAC World Congr., Preprints*, 1990, vol. 3, pp. 76–81.
- [9] A. Zhirabok and O. H. Preobrazhenskaya, "Robust fault detection and isolation in nonlinear systems," in *Proc. IFA C Symp. "Safeprocess'94,"* 1994, pp. 244–248.
- [10] *Control Valve Handbook*, Fisher Controls, 1977.
- [11] J. F. Davidson, R. Clift, and D. Harrison, Eds., *Fluidization*. New York: Academic, 1985.
- [12] M. Basseville and I. V. Nikiforov, *Detection of Abrupt Changes*. Englewood Cliffs, NJ: Prentice-Hall, 1993.
- [13] H. J. Marquez and C. P. Diduch, "Sensitivity of failure detection using generalized observers," *Automatica*, vol. 28, no. 4, pp. 837–840, 1992.
- [14] W. Birk and A. Medvedev, "Pressure and flow control of a pulverized coal injection vessel," in *Proc. 1997 IEEE Int. Conf. Contr. Applicat.*, 1997, pp. 127–132.



**Andreas Johansson** (S'98) was born in Luleå, Sweden, in 1972. He received the M.Sc. degree in computer science from Luleå University of Technology in April 1997. After graduation, he joined the Control Engineering Group of the university as a Ph.D. student.

His research interest is mainly in fault detection.

**Alexander Medvedev** was born in Leningrad (St. Petersburg), USSR (Russia), in 1958. He received the M.Sc. (honors) and Ph.D. degrees in control engineering from the Leningrad Electrical Engineering Institute (LEEI) in 1981 and 1987, respectively. In 1991, he received the docent degree from the LEEI.

From 1981 to 1991, he subsequently held positions as a System Programmer, Assistant Professor, and Associate Professor in the Department of Automation and Control Science at the LEEI. He was with the Process Control Laboratory, Åbo Akademi, Finland, during a research visit in 1990 to 1991. In 1991, he joined the Control Engineering Group (CEG) at Luleå University, Sweden, as an Associate Professor. In 1996, he was promoted to docent. From October 1996 to December 1997, he served as Acting Professor of automatic control and since January 1998, he has been a Full Professor at the CEG. His current research interests include fault detection, fault tolerance, time-delay and time-varying systems theory, and control applications.